6-24-2014

Sources and sinks of carbonyl sulfide in an agricultural field in the Southern Great Plains

Kadmiel Maseyk
Université Pierre et Marie Curie, kadmiel.maseyk@upmc.fr

Joseph A. Berry
Carnegie Institution, Stanford, CA, jberry@dge.stanford.edu

David P. Billesbach
University of Nebraska-Lincoln, dbillesbach1@unl.edu

John Elliott Campbell
Sierra Nevada Research Institute, University of California, Merced, CA, ecampbell3@ucmerced.edu

Margaret S. Torn
Lawrence Berkeley National Laboratory, mstorn@lbl.gov

See next page for additional authors

Authors
Kadmiel Maseyk, Joseph A. Berry, David P. Billesbach, John Elliott Campbell, Margaret S. Torn, Mark Zahniser, and Ulli Seibt

Sources and sinks of carbonyl sulfide in an agricultural field in the Southern Great Plains

Kadmiel Maseyk[a,1], Joseph A. Berry[b], Dave Billesbach[c], John Elliott Campbell[d], Margaret S. Torn[e], Mark Zahniser[f], and Ulli Seibt[a,g,1]

[a]Institute of Ecology and Environmental Sciences, Université Pierre et Marie Curie, Grignon Campus, 78850 Thiverval-Grignon, France; [b]Department of Global Ecology, Carnegie Institution, Stanford, CA 94305; [c]Biological Systems Engineering Department, University of Nebraska, Lincoln, NE 68583; [d]Sierra Nevada Research Institute, University of California, Merced, CA 95343; [e]Earth Sciences Division, Lawrence Berkeley National Laboratory, Berkeley, CA 94720; [f]Center for Atmospheric and Environmental Chemistry, Aerodyne Research Inc., Billerica, MA 01821; and [g]Department of Atmospheric and Oceanic Sciences, University of California, Los Angeles, CA 90095

Edited by Thure E. Cerling, University of Utah, Salt Lake City, UT, and approved May 14, 2014 (received for review October 10, 2013)

Net photosynthesis is the largest single flux in the global carbon cycle, but controls over its variability are poorly understood because there is no direct way of measuring it at the ecosystem scale. We report observations of ecosystem carbonyl sulfide (COS) and CO_2 fluxes that resolve key gaps in an emerging framework for using concurrent COS and CO_2 measurements to quantify terrestrial gross primary productivity. At a wheat field in Oklahoma we found that in the peak growing season the flux-weighted leaf relative uptake of COS and CO_2 during photosynthesis was 1.3, at the lower end of values from laboratory studies, and varied systematically with light. Due to nocturnal stomatal conductance, COS uptake by vegetation continued at night, contributing a large fraction (29%) of daily net ecosystem COS fluxes. In comparison, the contribution of soil fluxes was small (1–6%) during the peak growing season. Upland soils are usually considered sinks of COS. In contrast, the well-aerated soil at the site switched from COS uptake to emissions at a soil temperature of around 15 °C. We observed COS production from the roots of wheat and other species and COS uptake by root-free soil up to a soil temperature of around 25 °C. Our dataset demonstrates that vegetation uptake is the dominant ecosystem COS flux in the peak growing season, providing support of COS as an independent tracer of terrestrial photosynthesis. However, the observation that ecosystems may become a COS source at high temperature needs to be considered in global modeling studies.

carbonic anhydrase | LRU | ERU | flux partitioning | soil metabolism

Carbonyl sulfide (COS) is an atmospheric trace gas that holds great promise for studies of carbon cycle processes at regional to continental scales (1, 2). The drawdown of atmospheric CO_2 over the continents reflects the difference between terrestrial photosynthesis and respiration fluxes that are both substantially larger than the net CO_2 fluxes. This limits our ability to obtain information on gross fluxes from measurements of atmospheric CO_2 alone. On the other hand, the drawdown of atmospheric COS over the continents is thought to largely reflect photosynthetic fluxes (1, 3–6). At the global scale, the largest source of COS is the ocean, and uptake by leaves and soil are its largest sinks at 62% and 30% of the total sink, respectively (1).

The uptake of COS in leaves is due to hydrolysis catalyzed by the enzyme carbonic anhydrase (CA), resulting in production of H_2S and CO_2 (7). During leaf uptake, COS and CO_2 share the same diffusional pathway. The resulting close coupling of vegetation COS and CO_2 fluxes during photosynthesis (8–10) makes COS a promising tracer for gross carbon uptake where concurrent respiration precludes direct measurements of photosynthesis. For example, eddy covariance (EC) measurements of COS and CO_2 can be used to obtain independent estimates of gross primary productivity (GPP) at the ecosystem scale.

COS-based estimates of GPP are derived from ecosystem COS fluxes and the ratio of COS to CO_2 uptake during photosynthesis. Theoretical analysis (9, 11), laboratory studies of leaf-level COS and CO_2 exchange (10, 12–14), and initial ecosystem flux measurements (3, 4, 15) have confirmed the potential of this approach. However, uncertainty in some key assumptions remains to be addressed (3, 4, 11). The main assumptions behind this approach are that vegetation uptake is the dominant COS flux in land ecosystems and that soil or nonphotosynthetic fluxes are either minor or well characterized. The approach also requires knowledge of leaf relative uptake (LRU), the normalized ratio between COS and CO_2 fluxes during photosynthesis. LRU values have been measured in laboratory studies (9, 10, 12), but there is little information yet on the magnitude and variability of LRU under field conditions (15).

The enzyme CA is also assumed to be involved in COS hydrolysis by microbes in the soil (16, 17). Inhibitor (18) and isotopic studies (19, 20) indicate that CA is present in a range of soil types. A closely related enzyme, COS hydrolase, also decomposes COS but has little CO_2 hydration activity (21). Field measurements in Mediterranean, temperate, and boreal forests have typically shown COS uptake by soils, with higher rates (up to 13 pmol m^{-2} s^{-1}) observed in warmer ecosystems (22–24). Laboratory studies on soil COS exchange have shown COS consumption varies with temperature and water content but support the view that upland soils are generally a sink for COS (18, 25).

Soil COS emissions have also been observed and are usually associated with anoxic wetland soils (26, 27), but production from forest soils (28) and from wheat, forest, and paddy soils at higher temperature (29) has been reported. Nonwetland soil emissions suggest either a COS-producing process operating under aerobic conditions or production from anoxic microsites distributed in the soil profile (30).

Because most studies have used only periodic sampling, our knowledge of soil COS fluxes under field conditions remains limited. Consequently, laboratory data on one soil type (18) have

Significance

We report observations of ecosystem carbonyl sulfide (COS) and CO_2 fluxes that resolve key gaps in an emerging framework for using concurrent COS and CO_2 measurements to quantify terrestrial gross primary productivity. We show for the first time that leaf relative uptake ratios of COS and CO_2 during photosynthesis measured in the field vary systematically with light. We established that nocturnal COS uptake by vegetation is a significant component of daily net ecosystem COS fluxes. We also quantified a close correlation of soil COS fluxes with soil temperature. The small soil contribution to net ecosystem fluxes confirms that vegetation uptake is the dominant ecosystem COS flux in the growing season, a prerequisite for COS-based flux partitioning approaches.

Author contributions: K.M., J.A.B., D.B., J.E.C., M.S.T., and U.S. designed research; K.M., J.A.B., D.B., M.Z., and U.S. performed research; K.M., J.A.B., D.B., J.E.C., M.Z., and U.S. analyzed data; and K.M., J.A.B., D.B., J.E.C., M.S.T., and U.S. wrote the paper.

The authors declare no conflict of interest.

This article is a PNAS Direct Submission.

[1]To whom correspondence may be addressed. E-mail: kadmiel.maseyk@upmc.fr or useibt@ucla.edu.

This article contains supporting information online at www.pnas.org/lookup/suppl/doi:10.1073/pnas.1319132111/-/DCSupplemental.

been the basis for describing soil COS fluxes in regional and global analyses (2, 5, 6, 31). Recently, a more process-oriented approach incorporating the correlation of COS uptake rates with soil respiration observed in subtropical forest soils (32) was used in the simulation of global terrestrial COS fluxes (1). Thus, a better understanding of soil COS exchange is important to establish an independent, COS-based approach to obtain estimates of gross carbon fluxes from atmospheric or ecosystem measurements.

Here we report soil COS fluxes measured in a wheat field during spring–early summer 2012. We quantify the contribution of soil fluxes to net ecosystem COS fluxes that were measured concurrently by eddy covariance (15). From the soil and ecosystem flux data we obtain estimates of leaf relative uptake (LRU) and ecosystem relative uptake (ERU) needed to constrain terrestrial gross carbon fluxes at ecosystem to continental scales from COS and CO_2 measurements.

Results and Discussion

Soil COS Emissions and Uptake in a Wheat Field. Combining advanced instrumentation with an automatic soil chamber, we measured soil–atmosphere fluxes of COS near-continuously in a wheat field from April 4 to June 6, 2012 (Fig. 1 and Fig. S1). During the peak growing season [day of year (doy) 95–115], soil COS fluxes had diurnal variation between emissions and uptake (Fig. 1*B*). During the late season (doy 120–130), senescence (doy 135–145), and after harvest (after doy 145), soil fluxes shifted to emissions only, and the source strength and amplitude of the diurnal variation increased (Fig. 1*B*). Below, we will focus on the peak growing season first, followed by a discussion of the other phenological stages.

To evaluate the contribution of soil emissions to COS fluxes at the ecosystem scale, we compared our soil flux data with concurrent EC measurements of net ecosystem COS fluxes (15). Soil temperature in the cleared area around the chamber was often higher than that below the canopy (Fig. 1*C*). Therefore, we corrected our soil flux data to the below-canopy soil temperature (*Supporting Information*) to obtain soil COS flux estimates appropriate for comparison with net ecosystem fluxes.

We found that soil COS fluxes were minor compared with canopy uptake during the peak growing period, when net ecosystem COS uptake was high (Fig. 1*C*, doy 97–105). The average net ecosystem flux during this period was -26.2 ± 11.6 pmol m^{-2} s^{-1} ($n = 316$ 15-min periods), whereas the average soil flux was 1.6 ± 1.1 pmol m^{-2} s^{-1}. For daytime-only data, the average fluxes were -29.1 ± 10.5 and 1.7 ± 1.1 pmol m^{-2} s^{-1} ($n = 253$) for ecosystem and soil fluxes, respectively. Thus, soil emissions were <6% of net ecosystem COS uptake in this period. Our data confirm that vegetation uptake is the dominant ecosystem flux component during the peak growing season, satisfying the central requirement for COS-based NEE partitioning approaches (3, 4, 11).

Components of Leaf Relative Uptake. One of the applications of the COS tracer method is to obtain independent estimates of GPP from EC measurements of COS and CO_2 at the ecosystem scale. This is based on the LRU relationship between photosynthetic COS and CO_2 uptake (5):

$$\mathrm{LRU} = \frac{F_{\mathrm{COS}-vd}}{F_A}\frac{C_{a,c}}{C_{a,s}}, \qquad [1]$$

where F_A is the net photosynthetic carbon assimilation flux, $F_{\mathrm{COS}\text{-}vd}$ is the vegetation COS uptake during photosynthesis, and $C_{a,c}$ and $C_{a,s}$ are the atmospheric mole fractions of CO_2 and COS, respectively. F_A is related to gross photosynthesis as $F_A = \mathrm{GPP} - R_L$, where R_L is leaf respiration in the light. R_L is not well known but is typically small relative to GPP, and estimates of LRU to date have been based on measurements of F_A (9, 10). Furthermore, LRU has not been corrected for the influence of R_L when estimating GPP at ecosystem or larger scales (3–5), so we have maintained this approach here. During the day, plant COS uptake during photosynthesis ($F_{\mathrm{COS}\text{-}vd}$) and soil fluxes ($F_{\mathrm{COS}\text{-}sd}$) both contribute to net ecosystem fluxes of COS: $F_{\mathrm{COS}\text{-}ed} = F_{\mathrm{COS}\text{-}vd} + F_{\mathrm{COS}\text{-}sd}$.

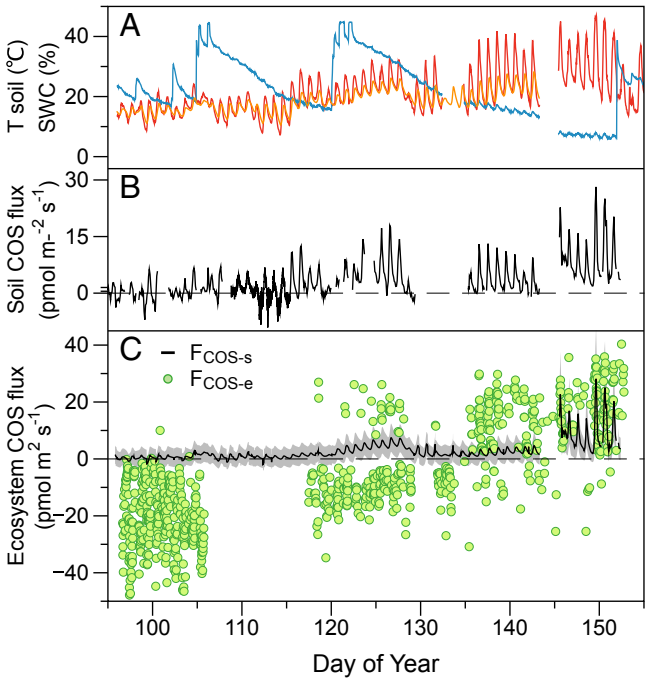

Fig. 1. Observed conditions and COS fluxes in a wheat field from April 4 to June 6, 2012. (*A*) Soil water content (SWC; blue) and temperature next to the chamber (red) and under the canopy (orange), (*B*) soil COS fluxes from soil chamber measurements, and (*C*) calculated at below-canopy soil temperature and SWC ($F_{\mathrm{COS}\text{-}s}$) and net ecosystem COS fluxes measured by eddy covariance ($F_{\mathrm{COS}\text{-}e}$) (15). In *C* the gray shading indicates the uncertainties in soil fluxes (*Supporting Information*). In *A*, there is a disconnect around day 145 because the sensors were removed and replaced for the harvest.

We calculated daily LRU values for 9 d during the peak of the growing season (doy 97–105) using ecosystem fluxes of gross photosynthesis and $F_{\mathrm{COS}\text{-}vd}$. For CO_2 fluxes, we used GPP estimates obtained from measured NEE (F_N) and ecosystem respiration (F_R) based on the traditional nighttime flux partitioning method [i.e., $\mathrm{GPP} = F_R - \mathrm{NEE}$ (33)]. In the following, ranges and averages are reported for doy 97–104 only. Values for doy 105 are listed separately because the weather was different on this day (overcast with rain). As the soil acted as a COS source during the day, $F_{\mathrm{COS}\text{-}vd}$ was on average 6% larger than $F_{\mathrm{COS}\text{-}ed}$ during this period. Daily LRU values ranged from 0.9 to 1.6, and 1.9 on doy 105, with a GPP-weighted LRU for the 8-d period of 1.3. These values are at the low end of the range of LRU reported previously [1.3–3.8 for crops (9) and 1.6–1.7 (12) and 1.6–2.0 for C_3 plants (10)] and were found to decrease with mean daily values of photosynthetically active radiation (PAR) (Fig. 2). This ecosystem-level response differs from the LRU light response measured in the laboratory (10, 12), which shows a rapid decline at low light levels and relative stability at PAR above ~200 μmol m^{-2} s^{-1} and contrasts with earlier studies that have used constant LRU to estimate GPP from COS data (e.g., refs. 3 and 5).

The relationship between LRU and PAR stems from the light dependency of CO_2 uptake. It reflects that LRU can be approximated as (9)

$$\mathrm{LRU} = R_{s-c}\left[\left(1+\frac{g_{s,\mathrm{COS}}}{g_{i,\mathrm{COS}}}\right)\left(1-\frac{C_{i,c}}{C_{a,c}}\right)\right]^{-1}, \qquad [2]$$

where $R_{s\text{-}c}$ is the ratio of stomatal conductances for COS vs. CO_2 (~0.83), $g_{s,\mathrm{COS}}/g_{i,\mathrm{COS}}$ is the ratio of stomatal to internal conductance

for COS uptake, and $C_{i,c}/C_{a,c}$ is the ratio of internal to ambient CO_2 mole fraction. As $g_{i,COS}$ includes the biochemical reaction rate of COS as a first-order constant (1), it may be a large component of the uptake pathway of COS in leaves. We expect systematic differences in $C_{i,c}/C_{a,c}$ between clear days with high average PAR and overcast days with low average PAR. As a conceptual example, on a clear day, a mean $C_{i,c}/C_{a,c}$ of 0.65 may result in a LRU of 0.9 if $g_{s,COS}/g_{i,COS} \sim 1.6$, whereas on a cloudy day, a mean $C_{i,c}/C_{a,c}$ of 0.8 may result in a LRU of 1.9 if $g_{s,COS}/g_{i,COS} \sim 0.8$. We also expect g_s to vary consistent with photosynthetic uptake rates driven by PAR; for example, $g_{s,COS}$ could be 0.2 on a clear day and 0.1 on a cloudy day. This would imply $g_{i,COS} \sim 0.12$ on both the clear and cloudy day; that is, there are no large variations in $g_{i,COS}$ required to explain the LRU variations. The LRU–PAR response could also be due to a light-dependent decrease in F_R, or COS production (see below) affecting $F_{COS\text{-}ed}$. However, LRU and GPP estimates are driven more by NEE than F_R (F_R = 14 ± 9% of GPP), and sensitivity tests indicate that uncertainty in F_R or COS emissions are unlikely to drive the LRU response. We therefore propose that light-driven variations in $C_{i,c}/C_{a,c}$ are the main reason for the observed LRU–PAR relationship. To interpret spatial and temporal variations in LRU, $g_{i,COS}$ needs to be quantified for a range of plant types and growth conditions. Although we found that LRU under field conditions was more variable (by a factor of 2) than previously assumed, it should be possible to construct similar scaling relationships as presented here to obtain LRU at larger scales. This is critical because, for example, using a constant LRU of 1.6 (from laboratory studies) instead of varying values of 0.9–1.9 (from our field data) would result in up to a 44% underestimation of GPP on clear days and a 19% overestimation of GPP on cloudy days from COS-based partitioning.

Components of Ecosystem Relative Uptake. Another promising application of the COS tracer is to analyze atmospheric measurements of COS and CO_2 to obtain GPP estimates at regional to continental scales. A useful parameter at these scales is ERU, expressing the relationship of the net ecosystem fluxes that are responsible for atmospheric COS and CO_2 variations (5):

$$\mathrm{ERU} = \frac{F_{COS-e}}{F_N}\frac{C_{a,c}}{C_{a,s}}, \qquad [3]$$

where $F_{COS\text{-}e}$ and F_N are the net ecosystem COS and CO_2 fluxes, respectively. In contrast to Eq. **1**, both fluxes in Eq. **3** can be obtained directly from EC measurements. ERU is also the ratio of the relative drawdown of atmospheric COS to CO_2 from vertical profile data (5). The daily ERU during the peak growing season from our ecosystem flux measurements was 3.3 ± 1.0 on average, ranging from 2.0 to 4.7, and 8.6 on doy 105. Our mean ERU is similar to values of 3.3–4.3 from the few other ecosystem measurements available (3, 4) and falls within the range of 2.6–4.5 obtained from atmospheric data over the midcontinent region of North America (1, 2, 5). This similarity provides evidence for the link between ecosystem fluxes and atmospheric drawdown and supports the value of COS as an observation-based tracer of photosynthesis at larger scales.

Similar to LRU, there is also a relationship between ERU and PAR (Fig. 2), but the slope is larger due to a relatively greater contribution from nighttime respiration to net daily CO_2 exchange during the days of low light and low photosynthesis. Calculating ERU for daytime (DT) only (Fig. 2) illustrates the relative effect of nighttime fluxes on the daily flux ratios. ERU DT is much closer to LRU at lower light than ERU and converges with LRU with increasing photosynthesis at higher light.

Nonphotosynthetic COS fluxes also contribute to the net flux and ERU values: $F_{COS\text{-}e} = F_{COS\text{-}vd} + F_{COS\text{-}vn} + F_{COS\text{-}sd}$, where $F_{COS\text{-}vn}$ is nighttime COS uptake by the vegetation (15). Averaged over 24 h, soil fluxes ($F_{COS\text{-}sd}$) account for even less of net ecosystem fluxes than during the daytime, only about 1%, because daytime sources are largely balanced by nighttime sinks. There was, however, substantial nighttime vegetation COS uptake, accounting for 29 ± 5% of daily net ecosystem fluxes. This additional sink was due to nocturnal stomatal conductance, which enabled COS uptake by wheat leaves at night. In contrast to CO_2, the COS reaction in leaves does not require light and therefore continues as long as stomata remain open. At our site, nocturnal stomatal conductance (g_s) was measured at 0.023 ± 0.005 mol m^{-2} s^{-1}, compared with a light-saturated g_s of 0.42 ± 0.03 mol m^{-2} s^{-1}. Because mean daytime g_s is lower than the light-saturated value and taking into account the small internal COS conductance as discussed above, we estimate a nighttime total conductance of about 16–23% of daytime values. It should be possible to find similar relationships between nighttime and daytime conductance, and hence COS uptake, for other ecosystems (34). It would also be interesting to investigate how widespread nocturnal stomatal conductance is, its role in ecosystem functioning, and how it responds to changes in biotic and abiotic conditions. In this respect, COS measurements could be an ideal method to study nocturnal stomatal conductance because, in contrast to water vapor, the concentration gradient driving the COS flux does not disappear at night.

Assuming that the atmospheric drawdown of both COS and CO_2 reflects terrestrial fluxes, ERU is equal to LRU * GPP/NEE if $F_{COS\text{-}e} \sim F_{COS\text{-}vd}$, i.e., plant uptake is the dominant flux (Eqs. **1** and **3**). The midcontinent region has extensive corn agriculture, and it was not clear whether the lower ERU of this region was due to a lower GPP/NEE ratio or a lower LRU of the C_4 plants (5). Our measurements indicate that in some midcontinent areas, C_3 agriculture may contribute to low ERU via low LRU values. In addition, GPP/NEE derived from our partitioned EC measurements were also somewhat lower, ranging from 1.5 to 2.4 (4.0 on doy 105) with an average of 1.9 ± 0.3. However, is ERU/LRU a good approximation of GPP/NEE? The average ERU/LRU at our site was 2.6, similar to continental-scale estimates of ERU/LRU and mid–growing season GPP/NEE ratios for crops from eddy flux studies (5) but about 37% larger than site GPP/NEE

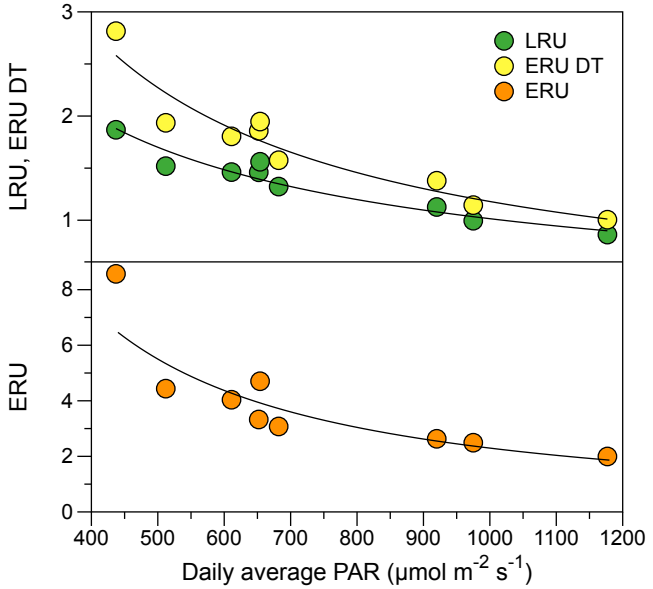

Fig. 2. Daily leaf relative uptake (LRU) and ecosystem relative uptake (daytime only, ERU DT; 24 h, ERU) vs. daily mean PAR during the main growing season (doy 97–105). LRU and ERU values were obtained from net ecosystem COS and CO_2 fluxes measured by eddy covariance (15), GPP values estimated using long-term nighttime respiration data from an adjacent AmeriFlux tower (33), and soil COS fluxes measured in the soil chambers. The fitted equations of the PAR–uptake ratio responses are LRU = 173.4 $PAR^{-0.744}$ (r^2 = 0.94, sd = 0.025), ERU DT = 844.4 $PAR^{-0.952}$ (r^2 = 0.93, sd = 0.034), and ERU = 13,833 $PAR^{-1.26}$ (r^2 = 0.85, sd = 0.067).

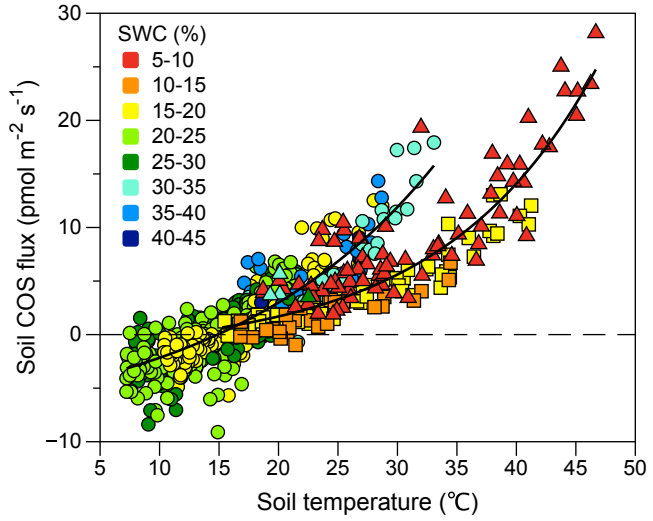

Fig. 3. Soil COS fluxes show a strong relationship with soil temperature, with a larger slope above SWC of ~20%. Data points are colored depending on SWC. Their shapes reflect phenological stages, with circles corresponding to the main growing season, squares corresponding to the senescence period, and triangles corresponding to the period after harvest. The fitted equations of the flux–temperature responses are $F_{COS} = -9.24 + 4.09e^{0.055 T_{soil}}$ ($r^2 = 0.74$, sd = 1.61) and $F_{COS} = -1.65 + 0.71e^{0.077 T_{soil}}$ ($r^2 = 0.82$, sd = 2.25) for the high and low SWC data, respectively.

due to nighttime COS uptake. Although nighttime uptake complicates the links between ERU, LRU, and GPP/NEE, nocturnal COS fluxes can be easily quantified from EC measurements, providing valuable information for both large-scale flux partitioning and studies of nighttime stomatal behavior.

Emissions Dominate Soil COS Fluxes in the Late Season. The second part of this paper explores the soil COS fluxes during the later phenological stages associated with grain filling, senescence, and harvest. Starting around doy 120, the increasing soil emissions (Fig. 1 *B* and *C*) are likely to complicate COS-based partitioning. After the harvest at doy 145, the source strength increased further. As very little residual biomass was left in place at this time, soil fluxes are expected to converge with ecosystem fluxes as the soil dominates net ecosystem exchange. There was good agreement between the soil fluxes measured with the chamber and net ecosystem fluxes measured by the EC system during this time (Fig. 1*C*; see also Fig. S2). Overall, the soil acted as both a sink and a source of COS, but emissions dominated during the latter part of the season. The soil was a net source of 360 μg S m^{-2} over the 2-mo period of our field campaign.

The soil COS fluxes in this system were strongly related to soil temperature over a 40 °C range, with a transition from sink to a source at ~15 °C (Fig. 3 and Fig. S3). Although soil COS fluxes were not directly correlated with soil water content (SWC, Fig. 1*A*), there appears to be a threshold for the COS flux vs. soil temperature response at a SWC of 15–20%, with a steeper slope at higher SWC (Fig. 3). SWC changes with season and plant phenological stage, and the data on the lower slope were predominantly associated with the senescence and postharvest period (after doy 130) that also had the highest temperature, reaching up to 46 °C (Fig. 3).

Daily Soil COS Fluxes Are Related to Daily CO_2 Fluxes. Soil CO_2 fluxes had similar—but weaker—correlations with soil temperature, including a similar SWC threshold (Fig. S4). A clear relationship between daily soil COS and CO_2 flux was evident when SWC was not limiting: daily fluxes were well correlated ($r = 0.81$) at SWC above 20% (Fig. 4). Both daily soil COS and CO_2 fluxes were high during times of high temperature combined with high SWC (e.g., around doy 125). In contrast, CO_2 fluxes decreased to near zero during periods of low SWC during senescence and harvest, whereas COS fluxes tended to remain high.

Below-Ground COS Production and Consumption. Our results show that both COS production and consumption processes are occurring in this soil, and the balance between the two processes is strongly temperature dependent. To investigate the origins of the COS fluxes, we measured different components inside the soil chamber sealed at its base: soil, roots, and grain heads (Fig. 5).

Soil was sampled from between the rows of wheat plants to avoid the main root system and measured in the chamber using an inert base. Because we kept the soil structure intact, some fine roots may have been present, but the samples were predominantly root-free. The soil samples were largely a sink but switched to a source later in the season when temperature was above 25 °C (Fig. 5*A*), i.e., a higher temperature than for the net soil fluxes. Most laboratory studies, typically conducted on sieved and root-free soil, show that soil under aerobic conditions is a net sink for COS due to the activity of soil microorganisms containing carbonic anhydrase or other CO_2-fixing enzymes (18, 25, 29). This type of soil COS uptake has a temperature optimum and tends to decline to zero at high (and low) temperature (18, 25, 29), consistent with an enzymatic process. On the other hand, COS emissions have been reported in some soils above 25 °C, including a wheat soil (29).

We also observed root-associated COS production (Fig. 5*B*). Freshly dug roots from the wheat plants were consistently found to emit COS at temperature between 12 and 30 °C. Production rates were greater at higher temperature later in the season, although a strong temperature response was not evident. The roots of four other species (*Lolium*, *Solanum*, and *Rumex* spp.) growing at the same location also all produced COS, suggesting that this might be a widespread phenomenon, but we are unable to say whether the COS is a product of root metabolism or rhizosphere microbial activity. COS production by the soil continued and was even stronger after harvest. We found that the root systems of plants that were cut above-ground at the end of March to install the chamber and measured in May continued to produce COS after the aboveground part of the plant had been removed, suggesting that decomposition or rhizosphere biota may also be involved. Postharvest COS emissions have been observed elsewhere in a wheat field (35) and in rice paddy soils (36). Net soil emissions of COS during spring have also been reported in a hardwood and a pine stand in Harvard Forest (28).

Above-Ground COS Production. In addition to the roots or associated microorganisms, brown wheat grain heads were also found to be producing COS (Fig. 5*B*). The grain heads had a near-zero

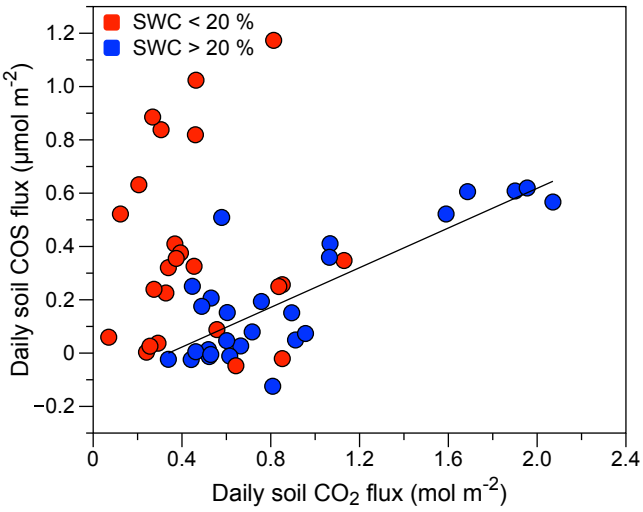

Fig. 4. Relationship between daily soil COS and CO_2 fluxes. Fluxes were well correlated at nonlimiting SWC: $F_{COS} = 0.359F_{CO2} - 1.373$ ($r = 0.81$) for SWC > 20%.

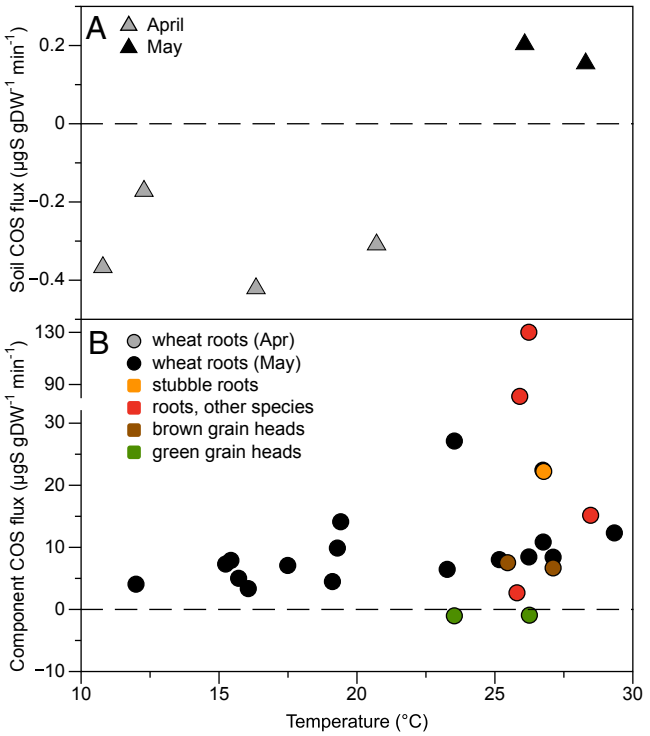

Fig. 5. COS production and uptake by root-free soil (*A*) and other components (*B*) measured in April and May: fresh wheat roots, wheat roots from plants that were cut at the end of March and measured in May (stubble), roots of other species growing on the edges of the wheat field, and the green and brown wheat grain heads.

COS flux when green but were producing COS when brown, near the end of the grain filling phase. Our ecosystem flux measurements also indicate above-ground net COS production. About 10 d before harvest, the whole ecosystem became a net source of COS at rates that greatly exceeded the soil fluxes (Fig. 1*B*). A study of COS exchange during germination, growth, and grain-filling phases in a wheat field in Germany also found the proportion of COS emissions increased with ontogenic development (37), with a compensation point for COS uptake that increased from about 160 ppt in spring to 500 ppt in summer. The capacity for above-ground plant COS production has also been documented in other species. For example, high COS compensation points were observed in a number of tree species, with occasional COS release in branch chambers at high temperature and in older leaves in autumn, indicating that emissions may be related to senescence processes (38). Canopy profile data from a loblolly pine forest indicated that the system was a source of COS to the atmosphere and more strongly from the canopy than the soil (39). COS emissions were also observed from plants in a salt marsh, although it is not clear whether the plants were acting as conduits for COS from the sulfate-rich anoxic soils or producing it themselves (27).

Potential Mechanisms of COS Production. COS production by soil, microbe or plant components is less well understood than uptake and may involve both biotic and abiotic processes (30). To date, the only known pathway of microbial COS production is through the hydrolysis of thiocyanate (40). The clear relationship between COS and CO_2 fluxes at high SWC earlier in the season (Fig. 4) suggests a strong biological component, and the lower sensitivity of COS flux to temperature under drier conditions and later in the season is consistent with physiological acclimation. On the other hand, there is little indication of a temperature optimum in the COS flux response (Fig. 3), particularly after harvest when the temperature exceeds 45 °C. The strong postharvest response suggests that an abiotic process, such as thermal degradation of organic matter as has been observed for CO production (41), may also be involved. Abiotic COS production may also explain why COS fluxes tended to remain high, whereas CO_2 fluxes decreased to near zero during periods of low SWC (Figs. 1 and 3).

Although the pathways of COS production are not well understood, plant S emissions are considered to be associated with the metabolism of S-containing amino acids (AAs), such as methionine and cysteine, and the regulation of cellular and organ S content with ontogenic development (42). There is a shift from S-rich leaf proteins to S-poor storage proteins during seed ripening in cereals, and significant internal redistribution of S occurs in wheat (43). The above-ground COS production we observed may therefore be related to the mobilization of S-containing AAs during grain-filling and leaf senescence. The overexpression of methionine precursors caused transgenic potato plants to shift from a sink to source of COS (44), providing more direct evidence that S-containing AA metabolism is involved in COS production. COS emissions were also observed following fungal infection in oilseed rape, suggesting a possible role in plant stress responses, and were associated with a decrease in total S, sulfate S, and cysteine (45).

The volatilization of S compounds also serves to regulate plant S levels when intake is in excess due to high soil or atmospheric levels (42). Fertilizer increases the production of S-containing AAs in wheat (43), and the metabolism or decomposition of these AAs may underlie increased COS emissions from fertilized soils (28, 35, 36, 46). The SGP site was fertilized during the season as part of typical agricultural practice.

The observed seasonal increase in above- and below-ground COS emissions from the SGP wheat field is thus probably due to a combination of several of these processes: (*i*) a temperature-driven decrease in the enzyme reaction rate and thus microbial COS uptake, (*ii*) a temperature-driven increase in COS released during organic matter degradation associated with microbial activity or abiotic processes, and (*iii*) a phenological or developmental related increase in plant COS production. These strong late season COS emissions do prevent it from being used as a tracer of GPP in this period, although photosynthesis is also low at this time. Further studies are needed to explore whether COS emissions are typical for certain ecosystems, environmental conditions, or phenological stages and to what extent they may confound COS-based estimates of GPP.

Outlook. The small contribution of soil fluxes to net ecosystem COS fluxes during the day is encouraging for the use of COS as a tracer for GPP at the ecosystem scale, particularly during the peak growing period, but GPP estimates can be improved by taking into account the light-dependence of LRU. To obtain GPP from atmospheric data at larger scales requires estimates of nighttime COS fluxes. Although measuring soil COS fluxes may not be necessary for COS-based partitioning, it would be useful for resolving how microbial activity and root metabolism operate together with microbial consumption to determine the overall soil COS flux dynamics. These processes differ in their temperature and SWC responses, are likely distributed differently in the soil profile, and may depend on the composition of the microbial community. Quantifications of the various processes across different ecosystems are exciting avenues for future research that would enhance not only our understanding of soil metabolism but also our ability to parameterize soil or nonstomatal COS fluxes in ecosystem and biosphere models. For example, we found evidence for both biological contribution to soil COS emissions at high SWC and abiotic production during periods of low SWC. This lends support to linking soil COS fluxes with soil heterotrophic metabolism (1) but also highlights the need to include production terms in future estimates of regional or global budgets, where nonwetland soil is currently only considered a COS sink (1, 31). Improving our model descriptions will be beneficial for exploring small-scale processes such as soil metabolism and nocturnal stomatal conductance as well as for simulations and inverse analyses of atmospheric COS and CO_2 data to obtain independent constraints on GPP at regional to global scales.

Methods

We conducted measurements of COS, CO_2, and water fluxes from April 4 to June 6, 2012 (doy 95–159), at the Atmospheric Radiation Measurement Southern Great Plains (SGP) Central Facility, near Billings, OK (36.61°N, 97.49°W). At the beginning of our field campaign, the wheat was ~30 cm tall on average. After harvest (May 20–22, doy 143–145), the campaign continued for another 2 wk of measurements over the bare soil.

Soils in the area are well-drained Kirkland (silt loam; fine mixed thermic Udertic Paleustolls), Renfrow (silty clay loam; a fine mixed thermic Udertic Paleustolls), and Vernon (clay loam; a clayey, mixed, thermic, shallow Typic Ustochrepts) associations, with a sand:silt:clay ratio of 33:22:45 ± 3 (33).

The soil flux measurements were made in conjunction with net ecosystem flux measurements of COS, CO_2, and H_2O using a portable EC tower (15) installed near a permanent EC tower (33). All gases were measured with a Quantum Cascade Laser (QCL) analyzer (CW-QC-TILDAS; Aerodyne Research Inc.). The 1s RMS noise (1 σ) of the instrument for COS is 5 ppt. Flow through the analyzer was provided by a TriScroll 600 pump (Varian, Inc.). All lines were 6-mm ID Synflex tubing (Eaton Hydraulics Group). Soil moisture and temperature of the upper 5 cm soil were monitored with a Hydra Probe II sensor (Stevens) adjacent to the soil chamber. The analyzer was housed in a climate-controlled shed at the base of the permanent EC tower.

We used a flow-through soil chamber (LI8100-104C) coupled to the QCL to measure soil fluxes of COS, CO_2, and water. The chamber was closed for 5 min every 2 h. During the closure periods, air was flowing through the chamber continuously at a flow rate of 5.1 slm, providing a turnover rate of $<1\ min^{-1}$. For every chamber measurement, we monitored the COS concentration of the incoming air for 1 min before and after the chamber closure. Fluxes were calculated from the difference between interpolated inlet concentration and the steady-state concentration in the chamber at the end of the closure period. The blank effects of the chamber and soil collar were characterized during two intensive measurement campaigns in April and May (*Supporting Information*).

ACKNOWLEDGMENTS. We thank the staff of the Department of Energy (DOE) Atmospheric Radiation Measurement Central Facility, particularly Pat Dowell, for hosting and assisting us in completing this project. We also thank two anonymous reviewers for their helpful comments and suggestions. This work was supported by the DOE, Biological and Environmental Research Division Award DE-SC0007094 and under Contract DE-AC02-05CH11231, European Research Council Starting Grant 202835 (to U.S.), and grants by the National Science Foundation Major Research Instrumentation program and the Air Liquide Foundation (to J.A.B.). Instrument development was supported by funding from the DOE, Small Business Innovation Research Grant DE-SC0001801.

1. Berry J, et al. (2013) A coupled model of the global cycles of carbonyl sulfide and CO_2: A possible new window on the carbon cycle. *J Geophys Res Biogeosci* 118(2):1–11.
2. Montzka SA, et al. (2007) On the global distribution, seasonality, and budget of atmospheric carbonyl sulfide (COS) and some similarities to CO_2. *J Geophys Res* 112(D9):D09302.
3. Asaf D, et al. (2013) Ecosystem photosynthesis inferred from measurements of carbonyl sulphide flux. *Nat Geosci* 6(3):186–190.
4. Blonquist JM, Jr., et al. (2011) The potential of carbonyl sulfide as a proxy for gross primary production at flux tower sites. *J Geophys Res* 116(G4):G04019.
5. Campbell JE, et al. (2008) Photosynthetic control of atmospheric carbonyl sulfide during the growing season. *Science* 322(5904):1085–1088.
6. Suntharalingam P, Kettle AJ, Montzka SM, Jacob DJ (2008) Global 3-D model analysis of the seasonal cycle of atmospheric carbonyl sulfide: Implications for terrestrial vegetation uptake. *Geophys Res Lett* 35(19):L19801.
7. Protoschill-Krebs G, Wilhelm C, Kesselmeier J (1996) Consumption of carbonyl sulphide (COS) by higher plant carbonic anhydrase (CA). *Atmos Environ* 30(18):3151–3156.
8. Goldan P, Kuster W, Albritton D, Fehsenfeld F (1987) The measurement of natural sulfur emissions from soils and vegetation: Three sites in the Eastern United States revisited. *J Atmos Chem* 5(4):439–467.
9. Seibt U, Kesselmeier J, Sandoval-Soto L, Kuhn U, Berry JA (2010) A kinetic analysis of leaf uptake of COS and its relation to transpiration, photosynthesis and carbon isotope fractionation. *Biogeosciences* 7(1):333–341.
10. Stimler K, Berry JA, Montzka SA, Yakir D (2011) Association between carbonyl sulfide uptake and $^{18}\Delta$ during gas exchange in C_3 and C_4 leaves. *Plant Physiol* 157(1):509–517.
11. Wohlfahrt G, et al. (2012) Carbonyl sulfide (COS) as a tracer for canopy photosynthesis, transpiration and stomatal conductance: Potential and limitations. *Plant Cell Environ* 35(4):657–667.
12. Stimler K, Montzka SA, Berry JA, Rudich Y, Yakir D (2010) Relationships between carbonyl sulfide (COS) and CO_2 during leaf gas exchange. *New Phytol* 186(4):869–878.
13. Sandoval-Soto L, et al. (2005) Global uptake of carbonyl sulfide (COS) by terrestrial vegetation: Estimates corrected by deposition velocities normalized to the uptake of carbon dioxide (CO_2). *Biogeosciences* 2(2):125–132.
14. Stimler K, Berry JA, Yakir D (2012) Effects of carbonyl sulfide and carbonic anhydrase on stomatal conductance. *Plant Physiol* 158(1):524–530.
15. Billesbach DP, et al. (2014) Growing season eddy covariance measurements of carbonyl sulfide and CO_2 fluxes: COS and CO_2 relationships in Southern Great Plains winter wheat. *Agric For Meteorol* 184:48–55.
16. Li W, Yu L, Yuan D, Wu Y, Zeng X (2005) A study of the activity and ecological significance of carbonic anhydrase from soil and its microbes from different karst ecosystems of Southwest China. *Plant Soil* 272(1-2):133–141.
17. Kato H, Saito M, Nagahata Y, Katayama Y (2008) Degradation of ambient carbonyl sulfide by *Mycobacterium* spp. in soil. *Microbiology* 154(Pt 1):249–255.
18. Kesselmeier J, Teusch N, Kuhn U (1999) Controlling variables for the uptake of atmospheric carbonyl sulfide by soil. *J Geophys Res* 104(D9):11577–11584.
19. Seibt U, Wingate L, Lloyd J, Berry J (2006) Diurnally variable $\delta^{18}O$ signatures of soil CO_2 fluxes indicate carbonic anhydrase activity in a forest soil. *J Geophys Res* 111(G4):G04005.
20. Wingate L, et al. (2009) The impact of soil microorganisms on the global budget of $\delta^{18}O$ in atmospheric CO_2. *Proc Natl Acad Sci USA* 106(52):22411–22415.
21. Ogawa T, et al. (2013) Carbonyl sulfide hydrolase from *Thiobacillus thioparus* strain THI115 is one of the β-carbonic anhydrase family enzymes. *J Am Chem Soc* 135(10):3818–3825.
22. Castro MS, Galloway JN (1991) A comparison of sulfur-free and ambient air enclosure techniques for measuring the exchange of reduced sulfur gases between soils and the atmosphere. *J Geophys Res* 96(D8):15427–15437.
23. Kuhn U, et al. (1999) Carbonyl sulfide exchange on an ecosystem scale: Soil represents a dominant sink for atmospheric COS. *Atmos Environ* 33(6):995–1008.
24. Simmons JS, Klemedtsson L, Hultberg H, Hines ME (1999) Consumption of atmospheric carbonyl sulfide by coniferous boreal forest soils. *J Geophys Res* 104(D9):11569–11576.
25. Van Diest H, Kesselmeier J (2008) Soil atmosphere exchange of carbonyl sulfide (COS) regulated by diffusivity depending on water-filled pore space. *Biogeosciences* 5(2):475–483.
26. de Mello WZ, Hines ME (1994) Application of static and dynamic enclosures for determining dimethyl sulfide and carbonyl sulfide exchange in Sphagnum peatlands: Implications for the magnitude and direction of flux. *J Geophys Res* 99(D7):14601–14607.
27. Whelan ME, Min D-H, Rhew RC (2013) Salt marsh vegetation as a carbonyl sulfide (COS) source to the atmosphere. *Atmos Environ* 73:131–137.
28. Melillo JM, Steudler PA (1989) The effect of nitrogen fertilzation on the COS and CS_2 emissions from temperate forest soils. *J Atmos Chem* 9(4):411–417.
29. Liu J, et al. (2010) Exchange of carbonyl sulfide (COS) between the atmosphere and various soils in China. *Biogeosciences* 7(2):753–762.
30. Conrad R (1996) Soil microorganisms as controllers of atmospheric trace gases (H_2, CO, CH_4, OCS, N_2O, and NO). *Microbiol Rev* 60(4):609–640.
31. Kettle AJ, Kuhn U, von Hobe M, Kesselmeier J, Andreae MO (2002) Global budget of atmospheric carbonyl sulfide: Temporal and spatial variations of the dominant sources and sinks. *J Geophys Res* 107(D22):4658.
32. Yi Z, et al. (2007) Soil uptake of carbonyl sulfide in subtropical forests with different successional stages in south China. *J Geophys Res* 112(D8):D08302.
33. Fischer ML, Billesbach DP, Berry JA, Riley WJ, Torn MS (2007) Spatiotemporal variations in growing season exchanges of CO_2, H_2O, and sensible heat in agricultural fields of the southern great plains. *Earth Interact* 11(17):1–21.
34. Caird MA, Richards JH, Donovan LA (2007) Nighttime stomatal conductance and transpiration in C_3 and C_4 plants. *Plant Physiol* 143(1):4–10.
35. Kanda K, Tsuruta H, Minami K (1995) Emissions of biogenic sulfur gases from maize and wheat fields. *Soil Sci Plant Nutr* 41(1):1–8.
36. Kanda K, Tsuruta H, Minami K (1992) Emission of dimethyl sulfide, carbonyl sulfide, and carbon bisulfide from paddy fields. *Soil Sci Plant Nutr* 38(4):709–716.
37. Kesselmeier J, Schröder P, Erismann JW (1997) Exchange of sulfur gasses between the biosphere and the atmosphere. *Biosphere-Atmosphere Exchange of Pollutants and Trace Substances, Transport and Chemical Transformation of Pollutants in the Troposphere*, ed Slanina S (Springer, Berlin), Vol 4, pp 167–198.
38. Geng C, Mu Y (2006) Carbonyl sulfide and dimethyl sulfide exchange between trees and the atmosphere. *Atmos Environ* 40(7):1373–1383.
39. Berresheim H, Vulcan VD (1992) Vertical distributions of COS, CS_2, DMS and other sulfur compounds in a loblolly pine forest. *Atmos Environ* 26(11):2031–2036.
40. Katayama Y, et al. (1992) A thiocyanate hydrolase of *Thiobacillus thioparus*. A novel enzyme catalyzing the formation of carbonyl sulfide from thiocyanate. *J Biol Chem* 267(13):9170–9175.
41. Conrad R, Seiler W (1985) Characteristics of abiological carbon monoxide formation from soil organic matter, humic acids, and phenolic compounds. *Environ Sci Technol* 19(12):1165–1169.
42. Rennenberg H (1991) The significance of higher plants in the emission of sulfur compounds from terrestrial ecosystems. *Trace Gas Emissions by Plants*, eds Sharkey TD, Holland EA, Mooney HA (Academic, San Diego), pp 217–260.
43. Zhao FJ, Hawkesford MJ, McGrath SP (1999) Sulphur assimilation and effects on yield and quality of wheat. *J Cereal Sci* 30(1):1–17.
44. Bloem E, et al. (2011) H_2S and COS gas exchange of transgenic potato lines with modified expression levels of enzymes involved in sulphur metabolism. *J Agron Crop Sci* 197(4):311–321.
45. Bloem E, Haneklaus S, Kesselmeier J, Schnug E (2012) Sulfur fertilization and fungal infections affect the exchange of H_2S and COS from agricultural crops. *J Agric Food Chem* 60(31):7588–7596.
46. Banwart WL, Bremner JM (1975) Formation of volatile sulfur compounds by microbial decomposition of sulfur-containing amino acids in soils. *Soil Biol Biochem* 7(6):359–364.

Supporting Information

Maseyk et al. 10.1073/pnas.1319132111

Field Site and Instrumentation

Measurements of soil carbonyl sulfide (COS), CO_2, and water fluxes were conducted at the Atmospheric Radiation Measurement Southern Great Plains (SGP) central facility, near Billings, north-central Oklahoma (36.61°N, 97.49°W), where eddy covariance (EC) measurements of ecosystem CO_2 and water fluxes are ongoing (see ref. 1). The field surrounding the EC tower was planted with winter wheat in January 2012. We conducted measurements from April 4 to June 6, 2012 [day of year (doy) 95–159]. There are two gaps in our datasets, due to an intensive field campaign (doy 130–135) and due to the harvest (around doy 145).

High-precision and high-resolution measurements of COS, CO_2, and H_2O were enabled by a Quantum Cascade Laser (QCL) analyzer (CW-QC-TILDAS; Aerodyne Research Inc.). The QCL analyzer produces a high-power, narrow line width beam that passes through a multipass absorption cell (2). An astigmatic Herriott cell provides a path length of 76 m in a 0.5 l volume. Measurements were made at a wavenumber of 2,050 cm^{-1}. Flow through the optical cell was provided by a TriScroll 600 pump (Varian, Inc.) at 6 slm and a pressure of 40 Torr, providing a cell turnover time of 0.166 s.

We used a flow-through soil chamber (LI8100-104C; Li-Cor) coupled to the QCL to measure soil fluxes of COS, CO_2, and water. The chamber was placed on a soil collar located inside the wheat field ∼30 m from the EC tower. The collar was inserted into the ground 6 d before the start of measurements to allow for any disturbance effects to settle. The residence time of air in the tubing between the chamber and QCL was 3–4 s. The air close to the soil was characterized by rapidly fluctuating COS concentrations. To supply the chamber with air containing a stable concentration of COS, the chamber inlet port was connected to tubing drawing air from an inlet at 4 m height on the adjacent EC tower. A three-way solenoid connected the QCL inlet to the chamber outlet line and the EC line.

For an estimate of spatial variability, measurements were made on two additional collars installed within a 20-m radius of the primary collar, also within the wheat field, between days 95 and 100. Fluxes from all three collars were measured within a half-hour period by moving the chamber between collars. Fluxes from the additional collars were correlated with the main primary collar ($r = 0.68$ and 0.82), and the difference between the mean of the three collars and the primary collar was -0.23 ± 2.50 pmol m^{-2} s^{-1} (mean ± SD, $n = 13$) over the set of replicate measurements.

Stomatal conductance was measured on the wheat plants at the site during peak growth at the start of the campaign (doy 92–98) using a LI-6400 portable photosynthesis system (Li-Cor, Inc.). Daytime measurements were made on 10 samples under saturating light and at a stable leaf chamber CO_2 concentration of 380 ppm. Nighttime measurements were made on 12 samples at least 1 h after dark.

Correcting Chamber Effects

The blank effects of the chamber and soil collar were characterized during two intensive measurement campaigns in April and May (Fig. S1) by sealing the bottom of the chamber with an inert base (FEP film; Goodfellow Cambridge Ltd.). Blank chamber tests were done on the automatic program and manually by actuating the chamber for repeated measurements within a short time period. We sometimes observed anomalously low (near zero) fluxes when the chamber was left overnight, which were attributed to condensation (data not shown and not included in regressions). This observation led us to also exclude some nighttime data from the soil flux measurements under similar conditions (with very low or negative water flux values).

We found temperature-dependent COS outgassing by both chamber and soil collar materials. There was good agreement between the two measurement dates and approaches. We derived exponential fits of COS production to the chamber air temperature and used this fit to correct the raw soil flux data. Separate equations were derived for the chamber only and chamber + collar (Fig. S1), and the collar-only effect was estimated by the difference. However, we note that a small bias in the exponential fit could lead to large errors in the flux correction as we extrapolate to very high temperatures (up to 46 °C) during the later parts of the campaign, outside the range of blank chamber measurements. The raw flux data were corrected for the two effects from chamber and collar materials separately. The effects of the chamber were scaled by air temperature. The effects of the collar cannot be scaled simply by soil temperature. This is because during the flux measurements about half of the collar height was inserted into the soil. Thus, the collar effects were scaled 50% each by air and soil temperature. On the other hand, the part of the collar that was inserted into the soil may not contribute fully to the chamber effects if some of its emitted COS is taken up within the soil. Thus, we used the above estimate as the upper limit and only the above-soil section of the collar as the lower limit of COS outgassing from the collar, with the best-estimate correction in between these two limits.

Soil and Ecosystem COS Exchange After Harvest

After harvest, when soil fluxes from the bare field are expected to dominate net ecosystem exchange, there was good agreement of the diurnal pattern and magnitude between the soil fluxes measured with the chamber and net ecosystem fluxes measured by the EC system (Fig. S2). The EC data also confirmed the strong soil source of COS after harvest at the site.

Increased Frequency Measurements

From doy 109–115, we increased the measurement frequency to 15 min (Fig. S3). This confirmed that the main diurnal variability was captured well by our regular 2-h cycle. The average COS flux during the 6 d was 0.53 ± 2.58 pmol m^{-2} s^{-1} for the 15-min data and 0.61 ± 2.45 pmol m^{-2} s^{-1} for the subset of data collected on the regular 2-hourly cycle. Total emissions over this period were 9.6 μg S m^{-2} and 11.2 μg S m^{-2} when calculated from the 15-min data and 2-hourly data, respectively. Average CO_2 fluxes at the two frequencies were within 1% of each other. The COS flux–temperature response does not change between the sampling frequencies (inset, Fig. S3), but there is more variability in the higher-frequency COS data, particularly at the higher uptake rates. The higher variability in the COS data is likely due to the lower precision of these measurements but may also indicate that the higher-frequency measurements were disturbing the soil profile more for COS than CO_2.

Relationship of COS, CO_2, and H_2O Fluxes with Soil Temperature

We found correlations between fluxes and soil temperature that varied with SWC (Fig. S4). For the COS flux, there appears to be a threshold for the soil temperature response between a SWC of 15–20%, with a steeper slope at higher SWC (Fig. S4*A*). However, phenological periods provide a clearer separation than a simple SWC response (Fig. 2). The relationships between CO_2 and water fluxes and soil temperature were similar to that of

COS fluxes but much more noisy (Fig. S4 *B* and *C*). The SWC threshold of CO_2 fluxes vs. soil temperature was also similar (Fig. S4*B*), although the effect of SWC on CO_2 fluxes was greater than for COS. Below the SWC threshold CO_2 fluxes increased with temperature during the first part of the campaign, whereas above the threshold CO_2 fluxes are small, with almost no change with temperature. This behavior started around doy 135 with low soil moisture and very high soil temperature (up to 46 °C). Evaporation was only weakly correlated with soil temperature (Fig. S4*C*). As the soil dried toward the end of the campaign, soil evaporation decreased and therefore did not simply reflect soil temperature.

Temperature Correction for Comparison of Soil and Net Ecosystem Fluxes

For a more appropriate ecosystem soil flux estimate we applied a temperature correction to the soil flux data. Some vegetation had to be cleared for chamber installation, and the temperature of the exposed soil in and around the collar was higher than that beneath the growing wheat canopy (Fig. 1*D*). Therefore, we corrected our measured soil fluxes to those of the below-canopy temperature using regressions obtained from the flux vs. soil temperature relationship (Fig. 2). Two flux–temperature relationships were derived, for SWC above and below 18%, and fluxes were estimated from temperature and SWC data measured beneath the undisturbed canopy as part of the regular ongoing site measurements. The correction was not applied to the postharvest data, when the canopy had been cleared. The total error on the corrected fluxes was determined by propagating the errors from the blank chamber corrections, the replicate chamber measurements, and the temperature corrections. Note that accounting for this correction results in a lower average LRU than the 1.6 presented earlier (3).

Soil COS Emissions

The total emissions estimated for the 7-wk measurement period up until harvest from below the canopy were 355 μg S m^{-2}. Emissions from the bare soil in the 2-wk period following harvest were 304 μg S m^{-2}. These estimates include some gap-filled fluxes using the 30-min soil temperature and SWC data and the observed temperature relationships.

We also estimated the soil COS fluxes for our site based on the approach typically used in regional and global budgets (4). The difference between our observations and this estimate amounts to an additional 820 μg S m^{-2} added to the atmosphere over the period of study.

1. Fischer ML, Billesbach DP, Berry JA, Riley WJ, Torn MS (2007) Spatiotemporal variations in growing season exchanges of CO_2, H_2O, and sensible heat in agricultural fields of the southern great plains. *Earth Interact* 11(17):1–21.
2. McManus JB, et al. (2010) Application of quantum cascade lasers to high-precision atmospheric trace gas measurements. *Opt Eng* 49(11):111124.
3. Billesbach DP, et al. (2014) Growing season eddy covariance measurements of carbonyl sulfide and CO_2 fluxes: COS and CO_2 relationships in Southern Great Plains winter wheat. *Agric For Meteorol* 184:48–55.
4. Kettle AJ, Kuhn U, von Hobe M, Kesselmeier J, Andreae MO (2002) Global budget of atmospheric carbonyl sulfide: Temporal and spatial variations of the dominant sources and sinks. *J Geophys Res* 107(D22):4658.

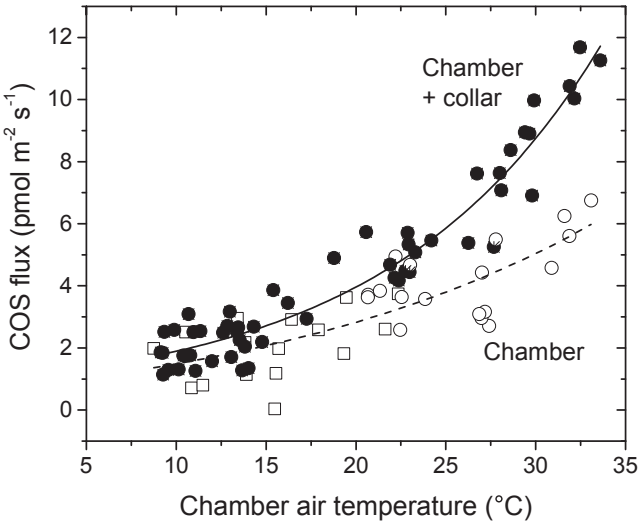

Fig. S1. COS produced by the chamber and soil collar depending on chamber air temperature. Tests were conducted in April (squares) and May (circles). Exponential regression curves were obtained from the chamber and chamber + collar data and used to correct measured soil fluxes: chamber flux = −1.75 + $2.51e^{0.031T}$ (r^2 = 0.62) and chamber + collar flux = 1.54 + $0.28e^{0.106T}$ (r^2 = 0.93), where T is temperature (°C).

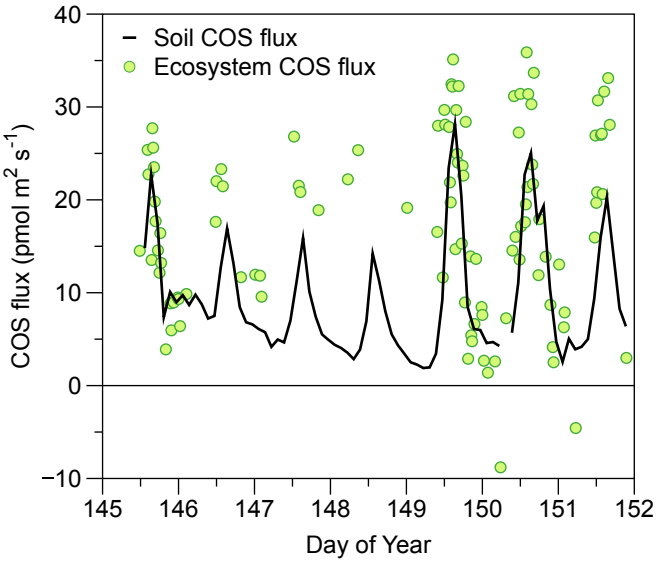

Fig. S2. Soil COS fluxes measured with the soil chamber agree well with net ecosystem fluxes measured by the EC system after harvest, when the soil dominates ecosystem fluxes. Note that this figure shows a detail from Fig. 1.

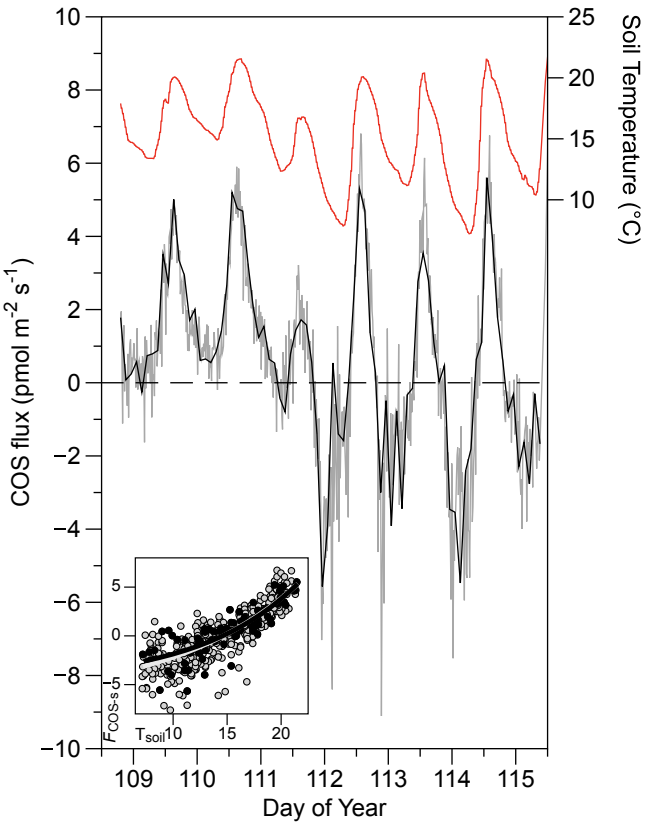

Fig. S3. Comparison of high-frequency soil measurements (15 min; gray line) to those on the regular 2-h cycle (black line) demonstrates that the regular 2-h schedule was able to capture the main diurnal variability of soil COS fluxes, which is strongly related to temperature (red line). The fitted equations of the flux–temperature response (inset) are $-6.82 + 2.00e^{0.0847Tsoil}$ ($r^2 = 0.71$, sd = 1.38) for the 15-min data (gray) and $-4.74 + 0.97e^{0.1097Tsoil}$ ($r^2 = 0.70$, sd = 1.33) for the 2-h data (Fig. 3). Note that this figure shows a detail from Fig. 1.

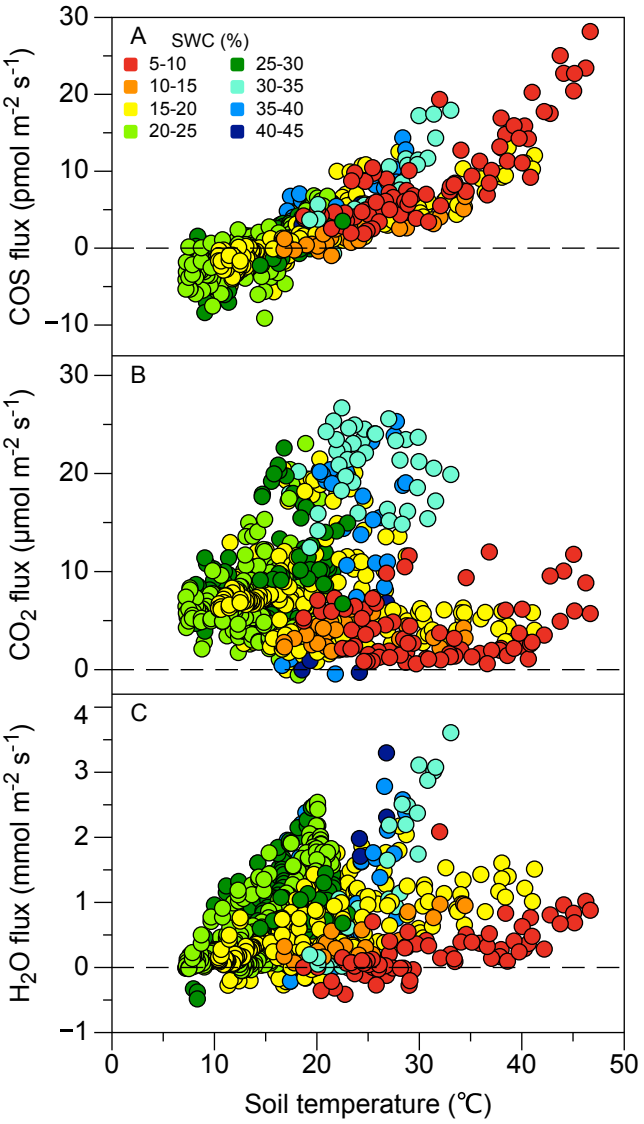

Fig. S4. Relationship between soil temperature and soil fluxes of COS (*A*), CO_2 (*B*), and water (*C*) depending on soil water content (SWC). The flux vs. temperature relationships have a threshold at SWC of 15–20%, with larger slopes above the threshold.